

A New FEM–BEM Coupling for the 2-D Laplace Problem

Jacques Lobry 

Department of General Physics, Faculty of Engineering, University of Mons, 7000 Mons, Belgium

A new hybrid finite element method–boundary element method (FEM–BEM) scheme is proposed for the solution of the nonlinear 2-D Laplace problem. The novelty is an original approach of the BEM where the domain integrals are eliminated at the discrete level by using the FEM approximation of the fundamental solution at every node of the related mesh in the linear regions. The implementation of this FEM–Green approach requires less computational burden than the standard BEM. The coupling with FEM is straightforward and appears to be more natural. The validity of the method is examined through numerical examples.

Index Terms—Boundary element method–finite element method (BEM–FEM) coupling, Green function, Laplace problem, nonlinear material.

I. INTRODUCTION

VARIOUS coupling strategies of the finite element method (FEM) and the boundary element method (BEM) have been developed to exploit the complementary advantages of both methods, i.e., the flexibility of the FEM for taking into account nonhomogeneous and nonlinear materials, and the natural ability of the BEM to consider unbounded domains, see e.g., [1], [2]. While the FEM is based on the Galerkin approximation of a weak or variation formulation, the standard BEM is generally deduced from the use of the second Green’s identity for reducing domain integrals into boundary ones [1].

In contrast to this classical approach, an alternative, *FEM–Green formulation*, is proposed for the BEM part of the coupling [3]. It is based on the FEM approximation of Green’s functions [4], and on the concept of nodal “cap” flux [5]. More precisely, the domain integrals of the actual BEM region are eliminated by combining the Galerkin formulation of the boundary value problem under study and the one associated with the fundamental solution for Dirac delta loading every node of a finite element mesh of this region. Only the finite elements directly connected to the boundary are actually required in order to well-define the nodal fluxes. The implementation of this new scheme requires less costly mathematical operations and the coupling with the standard FEM used in the FEM part is more natural. The method is applied to 2-D (in plane and axisymmetric) Laplace problems and is validated by some practical examples with open boundary and nonlinear domains.

II. MATHEMATICAL MODEL DESCRIPTION

The novelty of our FEM–BEM coupling concerns the BEM part that is used in the linear, possibly unbounded, domain we denote Ω_1 . The classical BEM formulation is replaced by an *FEM–Green formulation* consisting of a particular FEM treatment using the fundamental solution of the boundary value

Manuscript received November 24, 2020; revised February 5, 2021; accepted March 2, 2021. Date of publication March 8, 2021; date of current version May 17, 2021. Corresponding author: J. Lobry (e-mail: jacques.lobry@umons.ac.be).

Color versions of one or more figures in this article are available at <https://doi.org/10.1109/TMAG.2021.3064355>.

Digital Object Identifier 10.1109/TMAG.2021.3064355

0018-9464 © 2021 IEEE. Personal use is permitted, but republication/redistribution requires IEEE permission. See <https://www.ieee.org/publications/rights/index.html> for more information.

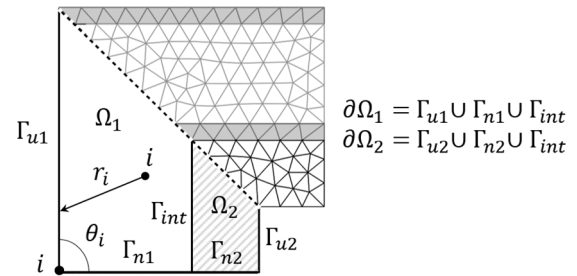


Fig. 1. General configuration for the 2-D Laplace problem and the FEM/FEM–Green treatment. Subdomains Ω_1 and Ω_2 are separated with the interface Γ_{int} .

problem. The domain integral is eliminated at the discrete level instead of using the second Green’s identity. First, we briefly recall the classical BEM. Then we will derive the FEM–Green formulation. The coupling with FEM applied to a nonlinear or nonhomogeneous region Ω_2 will be straightforward. The method is applied to the general configuration of the 2-D Laplace problem as depicted in Fig. 1.

A. Classical BEM

Due to a reduced mesh task and a natural open problem treatment capability, the BEM has been used for many years in mechanical and electrical engineering. In potential problems, the degrees of freedom are typically potential and normal derivative values are interpolated over the boundary elements. A system of linear equations is obtained for the unknowns at the boundary points. Then values of interest at internal points in the domain can be calculated separately.

Consider the Laplace equation defined on the domain Ω_1

$$\nabla^2 u = 0 \text{ in } \Omega_1, \text{ with } u = u_1 \text{ on } \Gamma_{u1} \text{ and } \frac{\partial u}{\partial n} = 0 \text{ on } \Gamma_{n1}. \quad (1)$$

The classical BEM formulation is based on the fundamental solution $\mathcal{G}_i = -1/2\pi \ln r_i$ of the governing equation, which is defined as

$$\nabla^2 \mathcal{G}_i = -\delta_i \text{ in } \Omega_1, \text{ with } \mathcal{G}_i = -\frac{1}{2\pi} \ln r_i \text{ on } \partial\Omega_1 \quad (2)$$

where δ_i is the Dirac delta function at any point i .

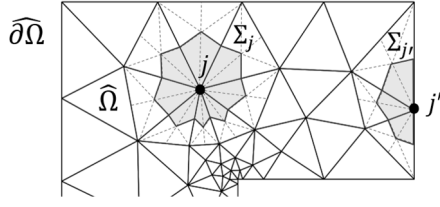


Fig. 2. Typical finite element triangular mesh and barycentric “box” Σ_j (“cap” Σ_j) for an internal (boundary) node j (j').

Using Green’s second identity applied to (1) and (2), the domain integrals are eliminated yielding

$$c_i u_i = \oint_{\partial\Omega_1} \left(u \frac{\partial \mathcal{G}_i}{\partial n} - \mathcal{G}_i \frac{\partial u}{\partial n} \right) d\Gamma. \quad (3)$$

The geometric factor c_i is equal to the ratio $\theta_i/2\pi$, where θ_i is the internal angle at node i , i.e., 1 at internal points and, e.g., 1/2 at boundary nodes in case of a smooth boundary. The discretization $\partial\widehat{\Omega}_1$ of the boundary $\partial\Omega_1$ into n elements Γ_j and n associated nodes i leads to the well-known statement

$$c_i \hat{u}_i = \sum_{j \in \partial\widehat{\Omega}_1} \int_{\Gamma_j} \frac{\partial \mathcal{G}_i}{\partial n} \hat{u} d\Gamma - \sum_{j \in \partial\widehat{\Omega}_1} \int_{\Gamma_j} \mathcal{G}_i \hat{q} d\Gamma \quad \forall i \in \partial\widehat{\Omega}_1 \quad (4)$$

where \hat{q} denotes the approximate normal derivative. The boundary potential \hat{u} and flux \hat{q} are typically interpolated linearly on every element Γ_j . The various integrals can be solved analytically or numerically. After prescribing the boundary conditions, the procedure leads to a consistent (fully populated) linear system of equations of which the solution consists of the unknown nodal values \hat{u}_i and \hat{q}_i .

B. FEM-Green Formulation

Consider now the Galerkin problem related to (1)

$$\int_{\Omega_1} \nabla \hat{u} \cdot \nabla N_j d\Omega = 0 \quad \forall j \in \hat{\Omega}_1 \setminus \hat{\Gamma}_{u1}, \hat{u} = u_1 \text{ on } \hat{\Gamma}_{u1} \quad (5)$$

where the N_j ’s are the classical interpolation functions defined on a finite element mesh $\hat{\Omega}_1$ of the domain Ω_1 (Fig. 2). The approximate solution \hat{u} is given by

$$\hat{u} = \sum_{k \in \hat{\Omega}_1} N_k \hat{u}_k. \quad (6)$$

On combining (5) and (6), a sparse system of linear equations is obtained, of which the matrix entries are found to be

$$s_{jk} = \int_{\hat{\Omega}_1} \nabla N_j \cdot \nabla N_k d\Omega. \quad (7)$$

When using linear elements, it is shown in [5] that the term

$$\Phi_{\hat{u}, \Sigma_j} = \int_{\hat{\Omega}_1} \nabla \hat{u} \cdot \nabla N_j d\Omega = \sum_{k \in \hat{\Omega}_1} s_{jk} \hat{u}_k \quad \forall j \in \hat{\Omega}_1 \quad (8)$$

is equal to the inward flux of $\nabla \hat{u}$ across the “box” Σ_j associated with node j in the dual mesh obtained from the barycentric subdivision of the primal 2-D mesh as shown in Fig. 2. Equation (5) means that those fluxes vanish for nodes $j \in \hat{\Omega}_1 \setminus \hat{\Gamma}_{u1}$ whereas they can be interpreted as the flux of $\nabla \hat{u}$

through “caps” associated with Dirichlet boundary nodes like $j' \in \hat{\Gamma}_{u1}$. In the following, the parameters $\Phi_{\hat{u}, \Sigma_j}$ are used in place of the approximation of the normal derivative \hat{q} given by the standard BEM.

As in the standard BEM, the 2-D fundamental solution \mathcal{G}_i of Laplace’s equation is employed in order to eliminate the domain integral. Due to its singularity of the solution, \mathcal{G}_i lies outside Sobolev space H^1 . However, an FEM solution does exist [4] and is readily derived from the Galerkin problem associated with the formulation (2)

$$\int_{\hat{\Omega}_1} \nabla \hat{\mathcal{G}}_i \cdot \nabla N_j d\Omega = \int_{\hat{\Omega}_1} \delta_i N_j d\Omega \quad \forall j \in \hat{\Omega}_1 \setminus \partial\widehat{\Omega}_1, \hat{\mathcal{G}}_i = \mathcal{G}_i \text{ on } \partial\widehat{\Omega}_1. \quad (9)$$

Again, the FEM solution $\hat{\mathcal{G}}_i$ is expressed as

$$\hat{\mathcal{G}}_i = \sum_{j \in \hat{\Omega}_1} N_j \hat{\mathcal{G}}_{i,j}. \quad (10)$$

For any *internal* node i of the mesh $\hat{\Omega}_1$, in the same way as for \hat{u} given by (8), we can write the nodal approximation

$$\Phi_{\hat{\mathcal{G}}_i, \Sigma_j} = \int_{\hat{\Omega}_1} \nabla \hat{\mathcal{G}}_i \cdot \nabla N_j d\Omega = \sum_{k \in \hat{\Omega}_1} s_{jk} \hat{\mathcal{G}}_{i,k} \quad \forall j \in \hat{\Omega}_1. \quad (11)$$

Note that we have $\Phi_{\hat{\mathcal{G}}_i, \Sigma_i} = 1$.

Using successively (5)–(8) and (10), we get

$$\begin{aligned} \int_{\hat{\Omega}_1} \nabla \hat{u} \cdot \nabla \hat{\mathcal{G}}_i d\Omega &= \sum_{j \in \hat{\Omega}_1} \left(\sum_{k \in \hat{\Omega}_1} s_{jk} \hat{u}_k \right) \hat{\mathcal{G}}_{i,j} \\ &= \sum_{j \in \hat{\Gamma}_{u1} \cup \hat{\Gamma}_{int}} \Phi_{\hat{u}, \Sigma_j} \hat{\mathcal{G}}_{i,j}. \end{aligned} \quad (12)$$

Conversely, using (6), adapted to $\hat{\mathcal{G}}_i$, (11) instead of (8), and the boundary conditions for u , we can write

$$\begin{aligned} \int_{\hat{\Omega}_1} \nabla \hat{\mathcal{G}}_i \cdot \nabla \hat{u} d\Omega &= \sum_{j \in \hat{\Omega}_1} \left(\sum_{k \in \hat{\Omega}_1} s_{jk} \hat{\mathcal{G}}_{i,k} \right) \hat{u}_j \\ &= \hat{u}_i + \sum_{j \in \hat{\Gamma}_{n1} \cup \hat{\Gamma}_{int}} \Phi_{\hat{\mathcal{G}}_i, \Sigma_j} \hat{u}_j + \sum_{j \in \hat{\Gamma}_{u1}} \Phi_{\hat{\mathcal{G}}_i, \Sigma_j} \hat{u}_1. \end{aligned} \quad (13)$$

Equating (12) and (13) yields the following expression:

$$\hat{u}_i + \sum_{j \in \hat{\Gamma}_{n1} \cup \hat{\Gamma}_{int}} \Phi_{\hat{\mathcal{G}}_i, \Sigma_j} \hat{u}_j + \sum_{j \in \hat{\Gamma}_{u1}} \Phi_{\hat{\mathcal{G}}_i, \Sigma_j} \hat{u}_1 = \sum_{j \in \hat{\Gamma}_{u1} \cup \hat{\Gamma}_{int}} \hat{\mathcal{G}}_{i,j} \Phi_{\hat{u}, \Sigma_j} \quad (14)$$

where the domain contribution is eliminated as expected.

In order to derive a consistent linear system of equations, (14) must now be written for all the nodes i belonging to the boundary $\partial\widehat{\Omega}_1$. Hence, the boundary condition of the problem (2) must be changed by introducing a Neumann condition in a neighborhood ε_i of i on $\partial\Omega_1$, such that $|\varepsilon_i| \rightarrow 0$

$$\mathcal{G}_i = -\frac{1}{2\pi} \ln r_i \text{ on } \partial\Omega_1 \setminus \{\varepsilon_i\} \quad \text{and} \quad \frac{\partial \mathcal{G}_i}{\partial n} = 0 \text{ on } \{\varepsilon_i\}. \quad (15)$$

So that the Galerkin formulation (9) is replaced by

$$\begin{aligned} \int_{\Omega_1} \nabla \hat{\mathcal{G}}_i \cdot \nabla N_j d\Omega &= \delta_{ij} c_i \quad \forall j \in (\hat{\Omega}_1 \setminus \widehat{\partial\Omega}_1) \cup \{i\}, \hat{\mathcal{G}}_i \\ &= \mathcal{G}_i \text{ on } \widehat{\partial\Omega}_1 \setminus \{i\} \end{aligned} \quad (16)$$

where δ_{ij} is the common Kronecker symbol and c_i is the same geometric factor as used in (3). From Gauss law at the discrete level, it can be easily shown that, in our FEM-Green context

$$c_i = \Phi_{\hat{\mathcal{G}}_i, \Sigma_i} \quad \text{and} \quad c_i + \sum_{j \in \widehat{\partial\Omega}_1 \setminus \{i\}} \Phi_{\hat{\mathcal{G}}_i, \Sigma_j} = 0. \quad (17)$$

Finally, the boundary element scheme amounts to solve simultaneously the n equations

$$\begin{aligned} c_i \hat{u}_i + \sum_{\substack{j \in \hat{\Gamma}_{n1} \cup \hat{\Gamma}_{\text{int}} \\ \neq i}} \Phi_{\hat{\mathcal{G}}_i, \Sigma_j} \hat{u}_j + \sum_{\substack{j \in \hat{\Gamma}_{u1} \\ \neq i}} \Phi_{\hat{\mathcal{G}}_i, \Sigma_j} \hat{u}_1 \\ = \sum_{j \in \hat{\Gamma}_{u1} \cup \hat{\Gamma}_{\text{int}}} \hat{\mathcal{G}}_{i,j} \Phi_{\hat{u}, \Sigma_j} \quad \forall i \in \widehat{\partial\Omega}_1 \end{aligned} \quad (18)$$

yielding unknown potential values \hat{u}_j and flux values $\Phi_{\hat{u}, \Sigma_j}$ depending on the boundary conditions.

At this point, the solution is the same as the one of (5) since (18) was derived by choosing test functions as a linear combination of the hat functions N_j in (12) and (13). However, in doing so, it would require the computation of the FEM approximations $\hat{\mathcal{G}}_i$ that is nonsense and highly time-consuming. Coefficients $\Phi_{\hat{\mathcal{G}}_i, \Sigma_j}$ and $\hat{\mathcal{G}}_i$ are then modified by using the *exact* fundamental solutions \mathcal{G}_i instead of $\hat{\mathcal{G}}_i$, i.e., the *interpolant*

$$\mathcal{G}_{i,I} = \sum_{j \in \hat{\Omega}_1} N_j \mathcal{G}_i(j) = - \sum_{j \in \hat{\Omega}_1} N_j \frac{1}{2\pi} \ln r_{ij} \quad (19)$$

where r_{ij} is the distance between nodes i and j . The infinite value $\mathcal{G}_i(i)$ is replaced by a value $\mathcal{G}_{i,i}^*$ that is derived by solving simultaneously the discrete Gauss laws (17), that is

$$\hat{c}_i = \sum_{k \neq i} s_{ik} \mathcal{G}_i(k) + s_{ii} \mathcal{G}_{i,i}^* \quad (20a)$$

and

$$\hat{c}_i + \sum_{j \in \widehat{\partial\Omega}_1 \setminus \{i\}} \left(\sum_{k \neq i} s_{jk} \mathcal{G}_i(k) + s_{ji} \mathcal{G}_{i,i}^* \right) = 0. \quad (20b)$$

In the same time, an estimate geometric factor \hat{c}_i is obtained.

Importantly, it is not necessary to mesh the whole domain when the interpolant $\mathcal{G}_{i,I}$ is used since the internal nodes are not involved in (18). A *single layer* of finite elements along the boundary $\widehat{\partial\Omega}_1$ (in light gray in Fig. 1) is sufficient. Any internal mesh of Ω_1 is used for field calculation at a preprocessing step.

The computational effort to build the linear system (18) scales as $\mathcal{O}(\epsilon)$ as in classical BEM. As no integration using a Gaussian quadrature is required to compute the modified coefficients $\Phi_{\hat{\mathcal{G}}_i, \Sigma_j}$, \hat{c}_i , $\mathcal{G}_i(j)$, and $\mathcal{G}_{i,i}^*$ of (18), a significant reduction in the computational burden is expected.

C. FEM/FEM-Green Coupling

In order to write the complete set of equations associated with the hybrid FEM/FEM-Green, the Galerkin problem related to the finite element domain Ω_2 must now be derived. By referring to Fig. 1, the governing equation is

$$\nabla \cdot k \nabla u = 0 \text{ in } \Omega_2, u = u_2 \text{ on } \Gamma_{u2}, \frac{\partial u}{\partial n} = 0 \text{ on } \Gamma_{n2} \quad (21)$$

where k is the nonhomogeneous or nonlinear material property of the region Ω_2 . The FEM problem is given by the equations

$$\int_{\hat{\Omega}_2} k \nabla \hat{u} \cdot \nabla N_j d\Omega = 0 \quad \forall j \in \hat{\Omega}_2 \setminus \hat{\Gamma}_{u2} \setminus \hat{\Gamma}_{\text{int}}, \hat{u} = u_2 \text{ on } \Gamma_{u2} \quad (22a)$$

$$\int_{\hat{\Omega}_2} k \nabla \hat{u} \cdot \nabla N_j d\Omega = -\Phi_{\hat{u}, \Sigma_j} \quad \forall j \in \hat{\Gamma}_{\text{int}}. \quad (22b)$$

The latter, (22b), expresses the flux continuity of $k \nabla \hat{u}$, across the interface, assuming $k=1$ in the BEM region for simplicity. Finally, the global system of algebraic equations of the whole problem is obtained by combining (18) and (22). It may be expressed as the partitioned matrix form

$$\begin{pmatrix} -\mathbf{G}_{11} & -\mathbf{G}_{1i} & \mathbf{H}_{11} & \mathbf{H}_{1i} & \mathbf{0} \\ -\mathbf{G}_{i1} & -\mathbf{G}_{ii} & \mathbf{H}_{i1} & \mathbf{H}_{ii} & \mathbf{0} \\ \mathbf{0} & \mathbf{1}_i & \mathbf{0} & \mathbf{S}_{ii} & \mathbf{S}_{i2} \\ \mathbf{0} & \mathbf{0} & \mathbf{0} & \mathbf{S}_{2i} & \mathbf{S}_{22} \end{pmatrix} \begin{pmatrix} \Phi_1 \\ \Phi_i \\ \hat{\mathbf{u}}_1 \\ \hat{\mathbf{u}}_i \\ \hat{\mathbf{u}}_2 \end{pmatrix} = \mathbf{b} \quad (23)$$

where the unknown vectors Φ_1 , and Φ_i refer to the nodal flux values on $\hat{\Gamma}_{u1}$ and $\hat{\Gamma}_{\text{int}}$, respectively, and $\hat{\mathbf{u}}_1$, $\hat{\mathbf{u}}_i$, and $\hat{\mathbf{u}}_2$ are related to the nodal potential values on $\hat{\Gamma}_{n1}$, $\hat{\Gamma}_{\text{int}}$, and $\hat{\Omega}_2 \cup \hat{\Gamma}_{n2}$, respectively. Global blocks \mathbf{H} and \mathbf{G} ($= \mathbf{G}^T$) represent the FEM-Green equations with the entries $\Phi_{\mathcal{G}_{i,I}, \Sigma_j}$ and $\mathcal{G}_i(j)$ or $\mathcal{G}_{i,i}^*$, respectively. Global block \mathbf{S} comes from the FEM contribution. As for most FEM/BEM coupling methods, this matrix has no special structure, i.e., neither symmetric nor positive definite. The right hand side \mathbf{b} relates to the Dirichlet boundary conditions.

III. NUMERICAL RESULTS

Two examples are presented to verify the validity of the proposed method and a comparison with classical techniques. All the algorithms were implemented in the MATLAB environment on a standard desktop computer. The lower-upper (LU) decomposition was used for the solution of the involved linear systems.

A. Example 1—Circular Coaxial Configuration

The first example is a linear Dirichlet problem defined on a circular coaxial configuration as depicted in Fig. 3. The field computation of this academic case is performed by using the FEM, the classical FEM/BEM coupling [1] and our FEM/FEM-Green method, respectively. In order to be general, a numerical integration (seven-point Gaussian quadrature) has been applied for the computation of the BEM integrals. Analytical integration could be applied [6], but it is not always possible as, e.g., in the axisymmetric case (see Section III-B). The global mesh size m has been considered as a parameter.

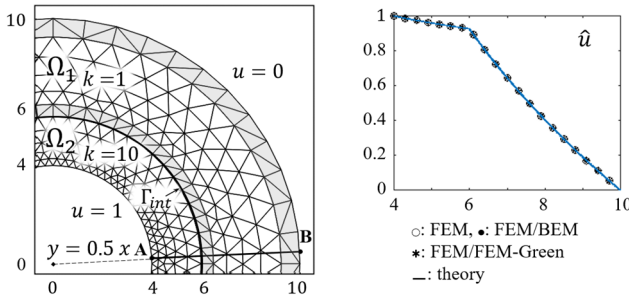


Fig. 3. Circular coaxial configuration and plot of \hat{u} along the line AB (dimensions in arbitrary units).

TABLE I
RELATIVE ERROR ON THE ENERGY

m	FEM	FEM/BEM	FEM/FEM-Green
1346	3.11×10^{-3}	3.14×10^{-3}	3.13×10^{-3}
5122	7.93×10^{-4}	8.01×10^{-4}	7.96×10^{-4}
18918	2.25×10^{-4}	2.29×10^{-4}	2.25×10^{-4}

TABLE II
MEASURED COMPUTATIONAL TIME (s) FOR $m = 18918$

FEM	FEM/BEM	FEM/FEM-Green
339.0	13.92	4.49

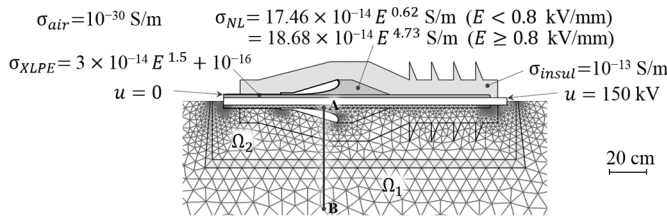


Fig. 4. Description of the dc cable termination and FEM/FEM-Green mesh.

The potential plot along the line AB is displayed in Fig. 3 for $m = 5122$. It demonstrates a very good agreement between all the methods. In a more quantitative way, Table I shows that the relative error in energy norm square, with respect to the analytical solution, is almost the same whatever the method. It is verified that it converges to zero as $\mathcal{O}(\uparrow^{-\epsilon})$.

Computational times shown in Table II clearly show a better performance of our method. It is due to far less mathematical operations involved in the computation of the coefficients occurring in submatrices \mathbf{H} and \mathbf{G} , with respect to the standard BEM, as can be seen by inspecting (18) and (11), see also [3]. Our approach remains competitive in case of analytical integrations by carefully comparing the number of operations [6].

B. Example 2–Cable Termination

The second example is more applicative. It deals with a dc cable termination with linear and nonlinear materials (Fig. 4) [7]. The problem is axisymmetric and the open boundary is taken into account in the implementation of our method. To simplify the implementation, the nonlinearity in the material property (conductivity σ) is treated here by simple iteration with underrelaxation for stability. The FEM-Green method is compared to FEM where a bounding box of radius R

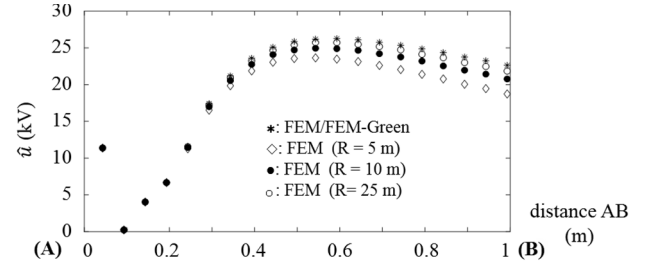


Fig. 5. Plot of the electric potential \hat{u} along the line AB.

with zero Dirichlet boundary condition is applied. The electric potential \hat{u} along the line AB is plotted in Fig. 5 for FEM with various R values and for FEM/FEM-Green. Convergence is observed as the box size increases in size, as expected. Again, the relative error ε in the resistive heating Q calculated in the solid insulating parts of the termination is very similar whatever the method, FEM/FEM-Green or FEM ($\varepsilon = 7.7 \times 10^{-3}$ for 1933 elements in the solid insulating parts, and the reference value is derived from a simulation with a very fine mesh). Comparing both methods, a reduction in CPU time is obtained with the FEM-Green, roughly by a factor of 5.

The axisymmetric fundamental solution is expressed in terms of complete elliptic integrals of the first kind [1]. An interest of our approach is that no complete elliptic integrals of the *second* kind are to be treated since the normal derivative of G is not involved, as it would be the case in classical BEM (not implemented here).

IV. CONCLUSION

The FEM/FEM-Green method presented in this article can take nonlinear material properties and open boundary problems into account, as other FEM/BEM coupling schemes usually do. An accuracy very close to other standard methods has been demonstrated. The advantages of the FEM-Green approach of the BEM part are a substantially reduced computational burden and a natural coupling with FEM, thanks to the cap flux concept. Our method can be extended to 3-D problems and higher order elements. However, in the latter case, the geometrical interpretation of the nodal flux is not so obvious as with the linear elements, but it remains a representative variable. Those aspects should be investigated in the future work.

REFERENCES

- [1] C. A. Brebbia, J. C. F. Telles, and L. C. Wrobel, *Boundary Element Techniques, Theory and Applications in Engineering*. Berlin, Germany: Springer, 1984, pp. 400–426.
- [2] E. P. Stephan, “Coupling of boundary element methods and finite element methods,” in *Encyclopedia of Computational Mechanics Fundamentals*, vol. 1. Hoboken, NJ, USA: Wiley, 2004, pp. 375–412.
- [3] J. Lobry, “A new boundary element formulation for the solution of Laplace’s equation,” in *WIT Transactions on Engineering Sciences*, vol. 126. Southampton, U.K.: WIT Press, 2019, pp. 63–73.
- [4] R. Araya, E. Behrens, and R. Rodríguez, “A posteriori error estimates for elliptic problems with dirac delta source terms,” *Numerische Math.*, vol. 105, no. 2, pp. 193–216, Nov. 2006.
- [5] A. Bossavit, “How weak is the ‘weak solution’ in finite element methods,” *IEEE Trans. Magn.*, vol. 34, no. 5, pp. 2429–2432, Sep. 1998.
- [6] J. Friedrich, “A linear analytical boundary element method (BEM) for 2D homogeneous potential problems,” *Comput. Geosci.*, vol. 28, no. 5, pp. 679–692, Jun. 2002.
- [7] F. Wang *et al.*, “Research on improving electric field distribution of cable terminal based on non-linear materials,” *IOP Conf. Ser., Earth Environ. Sci.*, vol. 153, May 2018, Art. no. 042044.